NASA TECHNICAL MEMORANDUM NASA TM 75277

INVESTIGATIONS OF THE INFLUENCE OF THE PROFILE THICKNESS OF THE COMPRESSIBLE PLANE FLOW THROUGH COMPRESSOR CASCADES

Jurgen Bahr

Translation of "Untersuchungen ueber den Einfluss der Profildicke auf die kompressible ebene Stroemung durch Verdichtergitter", Forschung im Ingenieurwesen Vol. 30 no.1 1964, pp. 14-25.

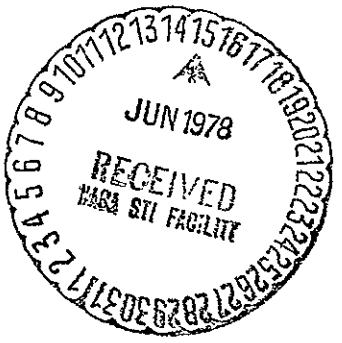

NATIONAL AERONAUTICS AND SPACE ADMINISTRATION
WASHINGTON, D. C. 20546 APRIL 1978

STANDARD TITLE PAGE

1. Report No. NASA TM 75277	2. Government Accession No.	3. Recipient's Catalog No.
4. Title and Subtitle Investigations of the Influence of the Profile Thickness of the Compressible Plane flow through Compressor Cascades		5. Report Date April, 1978
		6. Performing Organization Code
7. Author(s) Jurgen Bahr		8. Performing Organization Report No.
		10. Work Unit No.
9. Performing Organization Name and Address SCITRAN Box 5456 Santa Barbara, CA 93108		11. Contract or Grant No. NASw-2791
		13. Type of Report and Period Covered Translation
12. Sponsoring Agency Name and Address National Aeronautics and Space Administration Washington, D.C. 20546		14. Sponsoring Agency Code

15. Supplementary Notes

Translation of "Untersuchungen ueber den Einfluss der Profildicke auf die kompressible ebene Stroemung durch Verdichtergitter", Forschung im Ingenieurwesen, v. 30, N. 1, 1964, pp. 14-25.

16. Abstract

Investigation of profile thickness influence on compressible two-dimensional flow through compressor cascades; flow-through cascade of aircraft turbine compressor is studied experimentally over wide range of Reynolds numbers and subsonic Mach numbers; it was found that deterioration of flow properties due to decreasing Reynolds numbers is less noticeable on thin profiles than on thick ones; however, thick profiles are advantageous in compressors designed for efficient partial-load behavior because thick profiles have relatively large range of usable inlet-flow angles. 30 refs.

17. Key Words (Selected by Author(s))	18. Distribution Statement
	Unclassified - Unlimited

19. Security Classif. (of this report)	20. Security Classif. (of this page)	21. No. of Pages	22.
Unclassified	Unclassified	32	

NASA-HQ

INVESTIGATIONS OF THE INFLUENCE OF THE PROFILE THICKNESS ON THE COMPRESSIBLE PLANE FLOW THROUGH COMPRESSOR CASCADES

Jurgen Bahr* /14**

SUMMARY

Considering the special operational conditions of airplane turbine engines, we investigated the influence of the profile thickness on the flow processes in plane compressor blade cascades, over a wide range of Reynolds numbers and over the entire Mach number range of subsonic flow. The high velocity cascade wind tunnel of the German research facility for aerodynamics and space flight (DFL) made it possible to independently change both variables. From the results of wake measurements for determining the loss coefficients and the deflection, and from pressure distribution measurements, it becomes clear that there is a deterioration of the flow properties of blade cascades with decreasing Reynolds number for thin profiles, but it is much less than for thick profiles. This is especially true in the upper range of Mach numbers investigated. On the other hand, it is advantageous to use thick profiles when one requires a favorable partial load behavior of the compressor. This is because thick profiles have a relatively large "useful" incident flow angle range.

1. INTRODUCTION

The development of flow machines is continuously attempting to improve the performance density in the machines, especially because of their use in turbine engines. This led to an increase in the flow velocities up to close to the speed of sound. At such high velocities,

*Adliswil, Switzerland. Shortened version of a technical university dissertation at Braunschweig in 1962. Research supported by the German Research Association was performed at the Institute for Aerodynamics of the German Research Facility for Aerodynamics and Space Flight (DFL) under the supervision of Professor H. Schlichting. The author gave partial results about the work at the meetings of the "Aerodynamics" and "Engines" subgroups of the Scientific Association for Aerodynamics and Space Flight, (WGLR), on November 2 and 3, 1961, in Aachen.

** Numbers in margin indicate pagination in foreign text.

it is important to know the influence of the profile thickness on the flow in axial turbo machines. For example, the maximum throughput is for the most part determined by the profile thickness (blocking Mach number). From this point of view, one would have to use thin profiles in order to achieve the highest possible blocking Mach number. On the other hand, the high flow velocities require high flotation rates, which in turn requires a high strength of the blades, and therefore thick profiles. The profile thickness influences the flow considerably in the blade cascades at these very high velocities, but also over the entire subsonic range, as can be derived from measurements using single wings of various thicknesses in the subsonic range [1, 2].

It is difficult to make a theoretical analysis of an axial wheel, and experiments are also difficult. However, by unrolling single coaxial cylinder segments into several plane blade cascades, it becomes possible to analyze them more easily. They are also more suited for fundamental research.

Of the many publications on plane blade cascades in incompressible flow, we will mention several. L. J. Herrig and coworkers [3] discuss measurement results about the influence of profile thickness on plane compressor flows using NACA 65 series profiles. W. Held [4] established semi-empirical relationships for determining an optimum cascade for a given velocity triangle, and the profile thickness is also considered. Also, B. Eckert [5] gave similar information about the influence of the finite profile thickness. In all of these investigations, it was found that thin profiles are better in terms of losses and deflections, compared with thick profiles if the incident flow has no shocks. On the other hand, large deflections [3] are possible by using thick profiles. Several extensive American investigations about plane compressor flows using the NACA 65-series profiles were concerned with the influence of curvature [6-8], and skeleton line load [6]. A summary about the influence of the various cascade parameters was given by H. Schlichting [9].

In the range of compressible plane blade cascade flow, there are a number of publications. For example, there are publications about general experiments regarding the influence of Mach number [10-12], or methods for calculating pressure distributions in potential flow [13-16]. Systematic investigations about the influence of individual profile parameters for compressible flow have only been performed in

investigations of the influence of curvature [17].

In order to clarify the influence of profile thickness on the plane flow through compressor cascades, we carried out experiments over the entire subsonic range (incident Mach number $Ma_1 = w_1/a_1 = 0.30$ to 0.80, where w_1 is the incident flow velocity, and a_1 is the speed of sound in the incident flow). For Reynolds numbers $Re_1 = w_1 l/v_1 = 0.5 \times 10^5$ to 6×10^5 (where l is the blade chord and v_1 is the kinematic viscosity of the incident flow). The change in Re_1 is important for the following reasons. In fixed axial machines, especially in compressors, the Reynolds numbers which occur are above the critical Reynolds number because of the high velocity and the large air density near the ground, so that the blade boundary layers are completely turbulent*. In this case, the influence of the Reynolds number on the behavior of a blade cascade remains small [4, 5]. In aircraft engines, on the other hand, which operate primarily at high altitudes, that is, at low air densities, the Reynolds numbers are much smaller. From the diagram in [18], one can establish how the Reynolds number Re_1 changes with flight altitude and flight Mach number. For example, for a flight Mach number of 1.5 at a flight altitude of 23 km, the Reynolds number Re_1 in the engine is only about 10% of its value on the ground. If we assume $Re_1 = 5 \times 10^5$ for installations on the ground, then at high flight altitudes, one can count on Reynolds numbers of $Re_1 = 5 \times 10^5$. In the range of incident Reynolds numbers of $0.5 \times 10^5 < Re_1 < 5 \times 10^5$ there are considerable changes in the aerodynamic coefficients with Reynolds number (see for example [19]. Therefore, we expanded the described cascade investigations to this range of Re_1.

The Mach number range which occurs in the engine is between that of almost incompressible flow and the blocking Mach number ($Ma_1 = 0.2$ to about 0.9). Since in the upper Mach number range, the aerodynamic coefficients change very much with Mach number, as is known from single wings, there is an urgent requirement to investigate cascades using independent changes in Mach number and Reynolds number. /15

*With an incident flow velocity $w_1 = 260$ m/s ($Ms_1 = 0.80$), a blade chord of $l = 40$ mm and a kinematic air viscosity of $v_1 = 2.0 \times 10^{-6}$ m^2/s on the ground, the Reynolds number becomes $Re_1 = w_1 l/v_1 \approx 5 \times 10^4$.

In addition, at small Reynolds number the degree of turbulence of the flow has a substantial influence on the aerodynamic coefficients of a blade cascade. This was discussed in the publications by H. H. Hebbel [25].

In our investigations, we used slightly curved NACA-65 Series profiles [20], which have been developed in the United States for blades in axial compressors. The profiles only differ by their thickness. The entire program is structured into an experimental part (wake measurements and pressure distribution measurements) and a theoretical part (investigation of potential theory pressure distributions). For the most part, the influence of the profile thickness for constant cascade configuration and constant cascade division was investigated. In addition, we show briefly how the thickness influence differs when there is a change in the grid division ratio. In the high velocity cascade tunnel, [21, 22] which has often been described the wind velocity can be varied from 10 to 300 m/s, and at the same time the static pressure can be changed from 0.05 to 1.0 at, at any wind velocity. Therefore, it is possible to independently change Reynolds number and Mach number over the entire Reynolds number and Mach number range given above.

2. EXPERIMENTAL INVESTIGATIONS

2.1 Test Execution and Evaluation

2.11 Blade cascade, measurement programs, and test configuration: The measurements were performed using plane compressor cascades, made up of blades with the profiles NACA 65-604, 65-606, 65-608, 65-610, and 65-612 of the NACA 65 series [20]. Figure 1a to 1e shows the profiles used, which differ by their thicknesses of 4, 6, 8, 10, and 12% of the blade chord 1. The blades had a chord of $l = 60$ mm and a length (span) of $h = 300$ mm. They were used without turbulence producers.

The investigations were made for only one blade angle $\beta_s = 130°$, but for three division ratios $t/l = 0.75$, 1.00, and 1.25, according to Figure 2a through 2c (where t is the blade division). Most of the investigations were done for a division ratio of $t/l = 1.0$, for which the incident flow angle β_1 was changed over the entire useful range. In the case of cascades with the smaller and larger division ratio, the measurements extended only over one incident flow angle β_1 in the

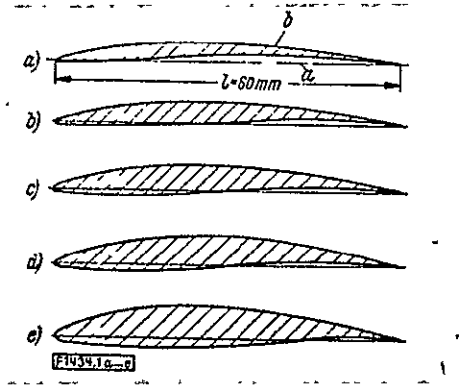

Figures 1a - 1c: Profiles used.

a- blade length b- profile l- blade chord
a) Profile NACA 65-604, b) Profile NACA 65-606
c) Profile NACA 65-608 d) Profile NACA 65-610
e) Profile NACA 65-612; the profile coordinates can be taken from [20].

range of incident flow directions without shocks. Table 1 gives the measurement program.

The measurement program included the following:

1. Wake measurements in the central section over one division t at a distance of $\bar{e}$ = 0.5 l = 30 mm from the cascade outlet plane, Figure 3;

2. Pressure distribution measurements on a profile contour in the center of the blade. We were able to produce pressure distribution measurement blades only for the three profiles with the maximum thicknesses of d = 0.08 l, 0.10 l and 0.12 l. The other profiles were too thin for this.

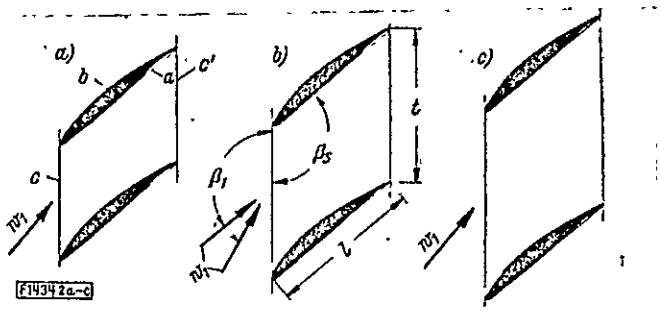

Figures 2a - 2c: Cascades Investigated.

a- blade length b- profile c- cascade front c'- trailing edge plane l- chord t- division, w_1- incident flow velocity, β_1- incident flow angle 140°, β_s- blade angle (for all cascades, 130°); a) cascades with t/l = 0.75, β_1 = 140°; b) cascades with t/l = 1 and β_1 = 130 to 150°, c) cascades with t/l = 1.25 and β_1 = 140°.

We measure the following variables (see Figure 3): stagnation pressure of incident flow $q_1 = p_{g1}$ (where p_{g1} is the total pressure, and p_1 is the static pressure of incident flow), the local total pressure loss $\Delta p_g(y') = p_{g_1} - p_{g_2}(y')$ (where $p_{g_2}(y')$ is the local total pressure in the wake measurement plane and y' is the coordinate parallel to it), the local static pressure difference $\Delta p(y') = p_2(y') - p_1$ with $p_2(y')$ as the local static pressure in the wake measurement plane, the local outlet flow angle $\beta_2(y')$ in the wake measurement plane, and the static pressure difference $p(x) = p_1$ along the profile contour (where p(x) is the static pressure on the profile contour at a distance x from the nose in the chord direction). The two-dimensional directional probes used in these wake measurements were described by U. Hopkes [11].

The degree of turbulence $T_u = \sqrt{\overline{u'^2}}/U$ of the cascade wind tunnel (where U is the average flow velocity, u' is the turbulent fluctuation velo- /15
city, and $\overline{u'^2}$ is the time average of u'^2) lies between 0.9 and 1.6% [24, 25] in the investigated Mach number and Reynolds number range. It is independent of the incident flow velocity and decreases with decreasing pressure level in the tunnel somewhat. The tunnel boundary layers, especially the side-wall boundary layers in the range of the cascade, were not sucked off. For a blade height ratio of h/l = 5, there is a sufficiently large range of about 3 to 4 l in the center of the cascade which is available. The static pressure p_1 of the incident flow, which is picked off at adjustable measurement points, was matched to the pressure of a static calibration probe before each wake measurement and the taps were located at a different distance of 1 blade chord ahead of the cascade shown in Figure 4. The cascades consisted of 7 or 9 blades, depending on the division ratio. In order to match the test configuration to the cascades with infinitely many blades, there were adjustable direction vanes at a distance of one-half of the division on the top and bottom sides of the cascade, which were curved according to the skeleton lines of the blade (see Figure 4). By turning these directional vanes around their rotation points, it was possible to equalize the static pressures p_o and p_u along the top and bottom floor to the static pressure p_1 of the incident flow.

2.12 Evaluation of measurements: The wake measurements were done using the momentum method of N. Scholz [23] (see Figure 3). In this method, which is well-known for a single profile, the inhomogeneous

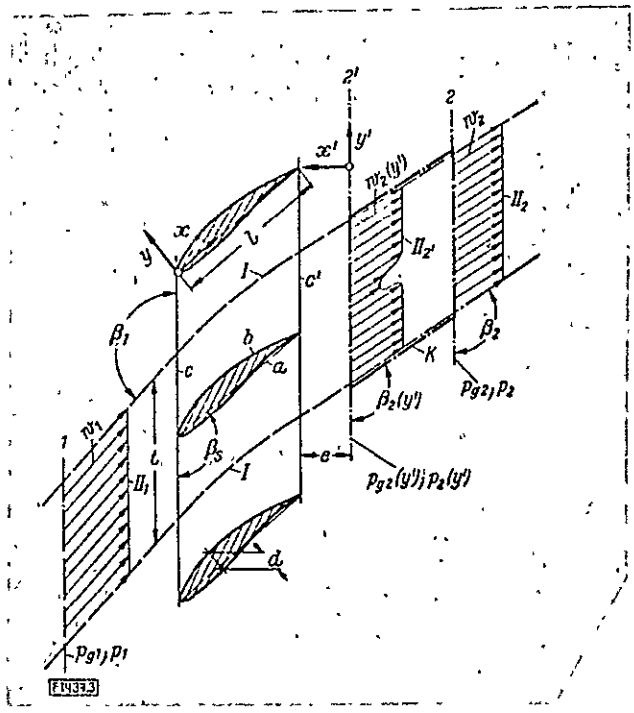

Figure 3: Notation for the blade cascade for evaluating wake measurements according to [23].

a- blade length b- profile c- cascade front c'- trailing edge plane (cascade exit plane) d- maximum profile thickness, l- blade chord, t- division, β_s- blade angle, x and y coordinates in the direction of the blade chord and perpendicular to it. I- central streamline between the blades, 1 plane for the undisturbed incident flow (velocity w_1), flow angle β_1, static pressure p_1, total pressure p_{g1}, velocity distribution II_1), 2 plane in the undisturbed outflow (velocity w_2, flow angle β_2, static pressure p_2, total pressure p_{g2}, velocity distribution II_2, 2' wake measurement plane at a distance e from the cascade outlet plane (velocity $w_2(y')$, flow angle $\beta(y')$, static pressure $p_2(y')$, total pressure $p_{g2}(y')$, velocity distribution II_2',) x' and y'- coordinates perpendicular to the plane 2', K control surface.

flow of the wake is calculated close to and behind the cascade, and from this one calculates the homogeneous flow very far behind the cascade using the momentum theorem. The final results of measurement are given for the homogeneous flow far behind the cascade. N. Schulz developed these momentum measurement methods for incompressible flow, but G. Kynast [26] showed that it can also be used for compressible flows in this form.

In compressor cascades, the aerodynamic coefficients are usually referred to the stagnation pressure q_1 of the incident flow. If p_g is the total pressure, and p is the stationary pressure, and if subscripts

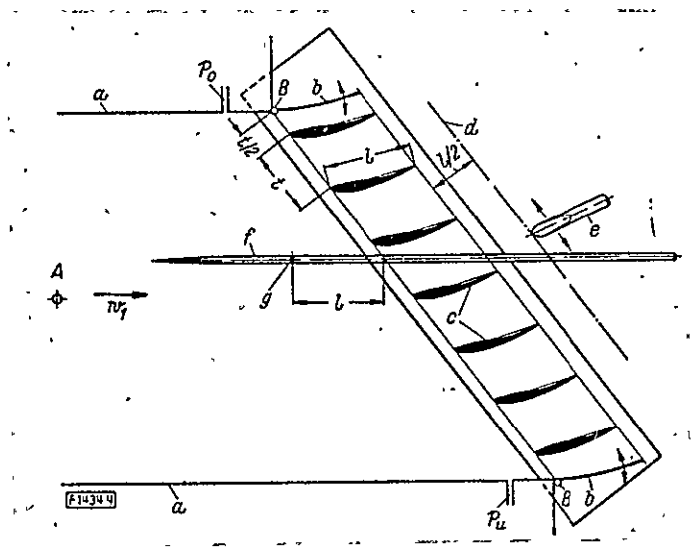

Figure 4: Diagram of Test Configuration

a- channel walls b- directive vanes c- cascade blades d- wake measurement planes e- wake probe (can be displaced parallel to d); f- static calibration probe g- static taps in probe A adjustable measurement point for static pressure p_2 of incident flow, B rotating point for the directive vanes, L blade chord t division, p_o and p_u static pressure at the top and lower channel walls ahead of cascade; w_1 flow velocity

Table 1: Measurement Program

Variable	Profile NACA				
	65-604	65-606	65-608	65-610	65-612
blade angle β_s	130°				
division ratio t/l	0,75, 1,0, 1,25				
incident flow angle β_1*	130° 135° 140°	130° 135° 140° 142,5° 145° 147°	130° 135° 140° 142,5° 145° 147°	130° 135° 140° 142,5° 145° 147° 150°	130° 135° 140° 142,5° 145° 147° 150°
incident Mach number Ma_1	0.30 to 0.60				
incident Reynolds no. Re_1	0,5 10^5; 1 · 10^5, 2 · 10^5, 4 · 10^5, 6 10^5				

*For t/l = 0.75 and 1.25, measurements only at β_1 = 140°.

**The investigations at $Re_1 = 6 \times 10^5$ were restricted because of the performance limits of the high velocity cascade wind tunnel and the strength of the blades. The results are substantially different from those at $Re_1 = 4 \times 10^5$. We will not present them here.

1 and 2 apply for the incident flow (plane 1 in Figure 3), and for the homogeneous outflow (plane 2), then the dimensionless total pressure loss is given by the following formula; that is, the total loss coefficient ζ_{v_1} referred to q_1:

$$\zeta_{v1} = \frac{p_{g1} - p_{g2}}{q_1} \tag{1}$$

and the dimensionless static pressure conversion is given by

$$\frac{\Delta p}{q_1} = \frac{p_2 - p_1}{q_1} \tag{2}$$

where $\Delta p = p_2 - p_1$. By integrating the local dimensionless total pressure difference $[p_{g1} - p_{g2}(y')]/q_1$ measured between plane 1 and the wake measurement 2' and by integrating the local dimensionless static pressure difference $[p_2(y') - p_1]/q_1$ over a division t, one first obtains the dimensionless average velocity total pressure loss

$$G = \frac{1}{t}\int_{y'}^{y'+t} \frac{p_{g1} - p_{g2}(y')}{q_1}\,dy' \tag{3}$$

and the dimensionless average static pressure difference

$$P = \frac{1}{t}\int_{y'}^{y'+t} \frac{p_2(y') - p_1}{q_1}\,dy' \tag{4}$$

The third wake measurement variable, the local outgoing flow angle $\beta_2(y')$, was only measured at several points outside of the wake depression. From these measured values, we calculated the average departing flow /17 angle β_{2m} using arithmetic averaging.

The recalculation of the average values G, P, and β_{2m} for homogeneous outgoing flow conditions very far behind the cascade (plane 2) is used in the correction quantity K, which was calculated universally by N. Scholz [23], and is given in a nomogram. One finally obtains the loss coefficient ζ_{v1}, the dimensionless static pressure conversion $\Delta p/q_1$, and the departing flow angle β_2 from the following equations:

$$\zeta_{v1} = G - K \tag{5}$$

$$\frac{\Delta p}{q_1} = P + 2K\sin^2\beta_{2m} \tag{6}$$

$$\operatorname{ctg}\beta_2 = \left(1 + \frac{K}{1 - P - G}\right)\operatorname{ctg}\beta_{2m} \tag{7}$$

Details of the calculation can be taken from [23].

The quantity ζ_{vl} is calculated using equations (3) and (5) with consideration of the blades in the cascade configuration. This loss coefficient therefore depends onthe division ratio t/l, even though the aerodynamic processes over the individual blades remain the same when t/l is changed. In order to analyze the influence of the profile thickness with variable division, it is appropriate to make the loss coefficient independent of the division ratio. By multiplying ζ_{vl} with the division ratio, we obtain the "fraction profile loss coefficient"

$$\zeta_{vpl} = \zeta_{vl}\frac{t}{l} \tag{8}$$

which corresponds to the drag coefficient c_w of an individual cascade blade [23, 26] (see also section 2.22). From the pressure distributions measured in the central section of the blade contour, we form the dimensionless pressure coefficient

$$c_p = \frac{p(x) - p_1}{q_1} \tag{9}$$

and then plot it as the function of the profile coordinate x/l. In order to determine the critical Mach number Ma_{1kr}, for which the speed of sound is reached at the blade contour, the critical pressure coefficient must be known (c_{pkr}). It is found according to [10] as follows

$$c_{pkr} = \frac{\left(\frac{2}{\varkappa+1} + \frac{\varkappa-1}{\varkappa+1}Ma_1^2\right)^{\frac{\varkappa}{\varkappa-1}} - 1}{\left(1 + \frac{\varkappa-1}{2}Ma_1^2\right)^{\frac{\varkappa}{\varkappa-1}} - 1} \tag{10}$$

and for a certain flow medium, depends on the ratio $\varkappa$ of the specific heats and the Mach number Ma_1 only.

2.2 Discussion of Measurement Results

2.21 General Remarks. Before we will discuss the influences of the profile thickness on the flow, through compressor cascades, we will make some general remarks regarding the influence of Mach number and

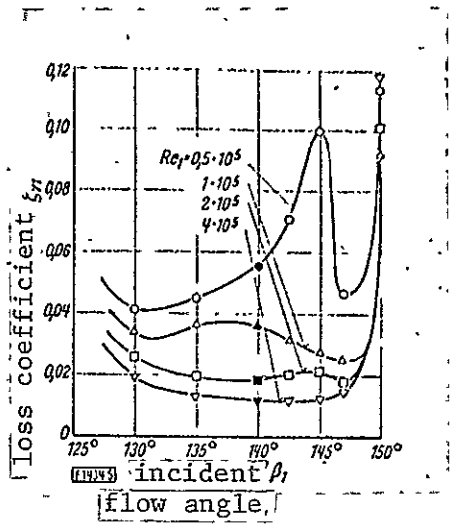

Figure 5: Influence of incident Reynolds number Re_1 on the cascade polar.

Cascades from blades with the profile NACA 65-612 with the blade angle β_s = 130° and the division ratio t/l = 1 for an incident Mach number Ma_1 = 0.3.

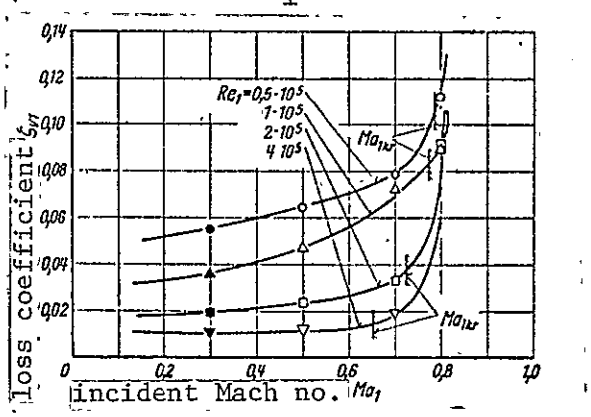

Figure 6: Influence of the incident Mach number Ma_1, on the loss coefficient ζ_{vl}, for different incident Reynolds numbers Re_1, for an incident angle of flow β_1 = 140° in the center of the polar. Cascade like in Figure 5; Ma_{1kr} is the critical incident Mach number.

Reynolds number on the boundary layer flow over blade profiles.

If we plot the loss coefficient ζ_{vl} of a cascade over the incident flow angle β_1, (cascade polar) for different Reynolds numbers, then it is found that ζ_{vl} in the Reynolds number range $0.5 \times 10^5 < Re_1 < 4 \times 10^5$ depends substantially on Re_1 as well as β_1. As the Reynolds number decreases, the losses increase, especially in the center of the polar, which is a region of incident flow without shocks.

The influence of the Mach number on the cascade losses can be seen in Figure 6. One can also see that the influence of the Mach number is great and depends greatly on Reynolds number. At high Reynolds numbers, ($Re_1 = 4 \times 10^5$), the increase of ζ_{vl} is relatively small in the

lower Mach number range, as Ma_1 increases. It is only in the vicinity of the critical Mach number that it is greater [11]. For small Reynolds number, the loss increase starts already at small Mach numbers, far away from the critical Mach number. The relatively great influence of Ma_1 and Re_1 on the flow through a blade cascade below the critical Mach number is based onprocesses in the blade boundary layer. We mean primarily boundary layer separations. The dependence of the non-separated boundary layer on Ma_1 and Re_1 (see [27]) can be ignored in this discussion. Three different kinds of boundary layer separation occur: 1. Separation of the laminary boundary layer, 2. Separation of the laminar boundary layer with turbulent reattachment 3. Separation of turbulent boundary layer. The processes during complete separations according to 1. and 3. are known according to [27]. In the case of the so-called separation bubble, according to 2., this is a special form of transition from laminar to the turbulent boundary layer [28]. Figure 7 is a diagram of the structure of such a bubble. It assumes a laminar incident boundary layer, and it separates from the blade as the pressure /18 increases. The separator boundary layer becomes turbulent and reattaches to the blade again.

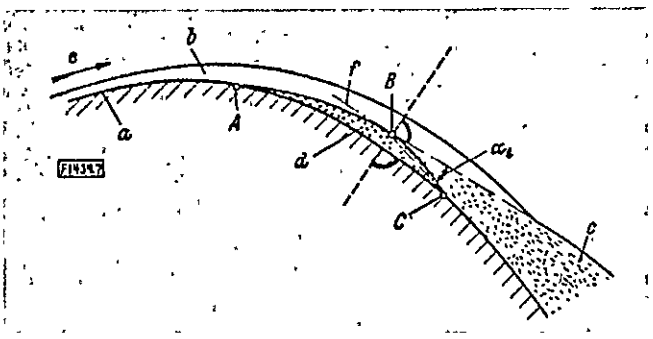

Figure 7: Schematic (non-scaled) design of a laminar separation bubble. a) body contour b, c) laminar and turbulent boundary layers, d) separation bubble e) flow direction f) tangent at the separation parallel to body contour, A separation point, B beginning of transition in boundary layer to the turbulent state, C position of reattachment α_t, angle of turbulent jet propagation.

The dependence of the laminar separation bubble on the Mach number and Reynolds number is determined by the manner in which the separation point and the reattachment point depend on these two variables. The

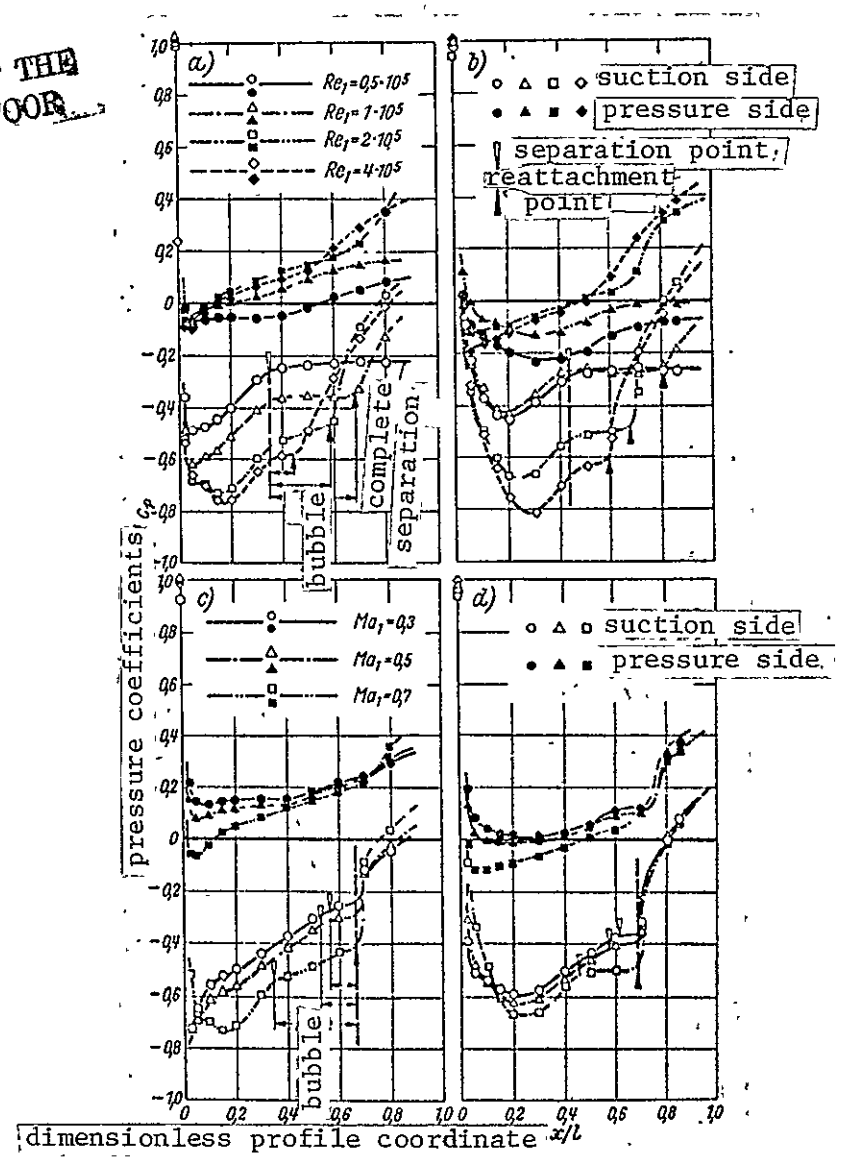

Figure 8a – 8d: Influence of incident Reynolds number Re_1 and incident Mach number Ma_1 on the pressure distribution around the profile characterized by the pressure coefficient c_p given by equation (9). Division ratio t/l, blade angle $\beta_s = 130°$, incident flow angle Re_1;

a), b) curves with Reynolds number Re_1 as the parameter at $Ma_1 = 0.7$ for the cascades made up of blades with a profile NACA 65-608 or NACA 65-612, c), d) curves with Mach no. Ma_1 as a parameter at $Re_1 = 2 \times 10^4$ for the cascade made up of blades with a profile NACA 65-608 or NACA 65-612.

calculation of the laminar boundary layer for a lifting profile for compressible subsonic flow using the method of E. Gruschwitz [29] showed [27] that the separation point migrates upstream somewhat with increasing Mach number. On the other hand, the Reynolds number has no influence on

the position of the separation point. Both results are confirmed by the new measurements shown in Figures 8a through 8d, which is an example of pressure disributions of two compressor cascades with profiles of various thickness, once with the Reynolds number, and once with the Mach number as a parameter.

A simple law was found for the reattachment point, and this point cannot be derived theoretically (see for example Figures 8a through 8d). It is independent of the Mach number, and with increasing Reynolds number it is displaced somewhat upstream. Since the transition point, which lies ahead of the reattachment point, cannot be derived from the pressure distributions, is directly related to the reattachment point and the neutral point*, this experimental result agrees with the result of theoretical calculations of the neutral point [27]. Accordingly, the Mach number only has a very small influence on the neutral point in the case of an impermeable wall, and it moves upstream with increasing Reynolds number. This means that as Mach number increases and Reynolds number decreases, a laminar separation bubble becomes larger, and in this way increases the profile losses.

2.22 Influence of Profile Thickness on Losses: According to the previous discussion, one should expect a great deal of dependence of the profile thickness influence on Mach number and Reynolds number. Figures 9a through 9t show the results in the form of cascade polars (loss coefficient ζ_{v1} plotted against β_1) where the profile thickness is a parameter, or the profile used) for different Mach numbers and Reynolds numbers. This shows the following:

1. The polars become wider with increasing profile thickness, especially the right branch of the polar; that is, for large incident flow angles (large load on the cascade).

2. The losses in general increase with increasing profile thickness.

*The neutral point of a laminar boundary layer flow is the point on the body in the flow where the Reynolds number formed with the path length or boundary layer thickness reaches a value which indicates laminar flow according to the stability limit theory. Above this critical Reynolds number, the boundary layer is unstable, and can be transferred into the turbulent state under certain conditions.

3. The loss increase with profile thickness depends on the incident flow angle and reaches especially high values in the center of the polar (in the region of incident flow direction without shocks).

4. With decreasing Reynolds number, and increasing Mach number, the influence of the profile thickness on the losses increases.

From the results of the smallest Mach number $Ma_1 = 0.30$, we will discuss the circumstances which will determine the variation of the polars. We already pointed out that the Reynolds number is very important in these processes. For the largest Reynolds number $Re_1 = 4 \times 10^5$, the polars differ only by the increasing width as the profile thickness increases. For smaller Reynolds numbers $Re_1 = 2 \times 10^5$, in addition /19 there is an increase in the losses in the center of the polar as the profile thickness increases. For $Re_1 = 1 \times 10^5$, this influence is even greater. For the smallest Reynolds number $Re_1 = 0.5 \times 10^5$, it is the most pronounced.

Losses like this in the center of the polar, which is the region of the incident flow angle which is usually the most favorable and has no shocks, are based on separation phenomena of the laminar boundary layer. Either there is a complete separation or a separation bubble (laminar separation with turbulent reattachment, as already discussed in section 2.21).

At $Re_1 = 4 \times 10^5$, the Reynolds number of the outer flow is so great that the boundary layer transfers at the correct time and for the most part there is no separation of the formation bubbles. The polars differ only in terms of width, but the boundary layers in the central polar region are not completely turbulent at this Reynolds number*. It is only for large incident flow angles that the suction side boundary layer undergoes transition already at the profile nose, because of the large suction peaks, whereas the boundary layer at the bldde pressure side is still laminar here. The increase in the losses on the right polar branch, which starts already for small incident flow angles for thin profiles, must be attributed to the completely turbulent boundary layer on the blade suction side, which always will bring about higher loss coefficients than a partially turbulent boundary layer with a laminar feed part, even though no or very small separation bubbles are formed.

*The critical Reynolds number of the investigated profiles is above 4×10^5 for the degree of turbulence of the high velocity cascade wind tunnel.

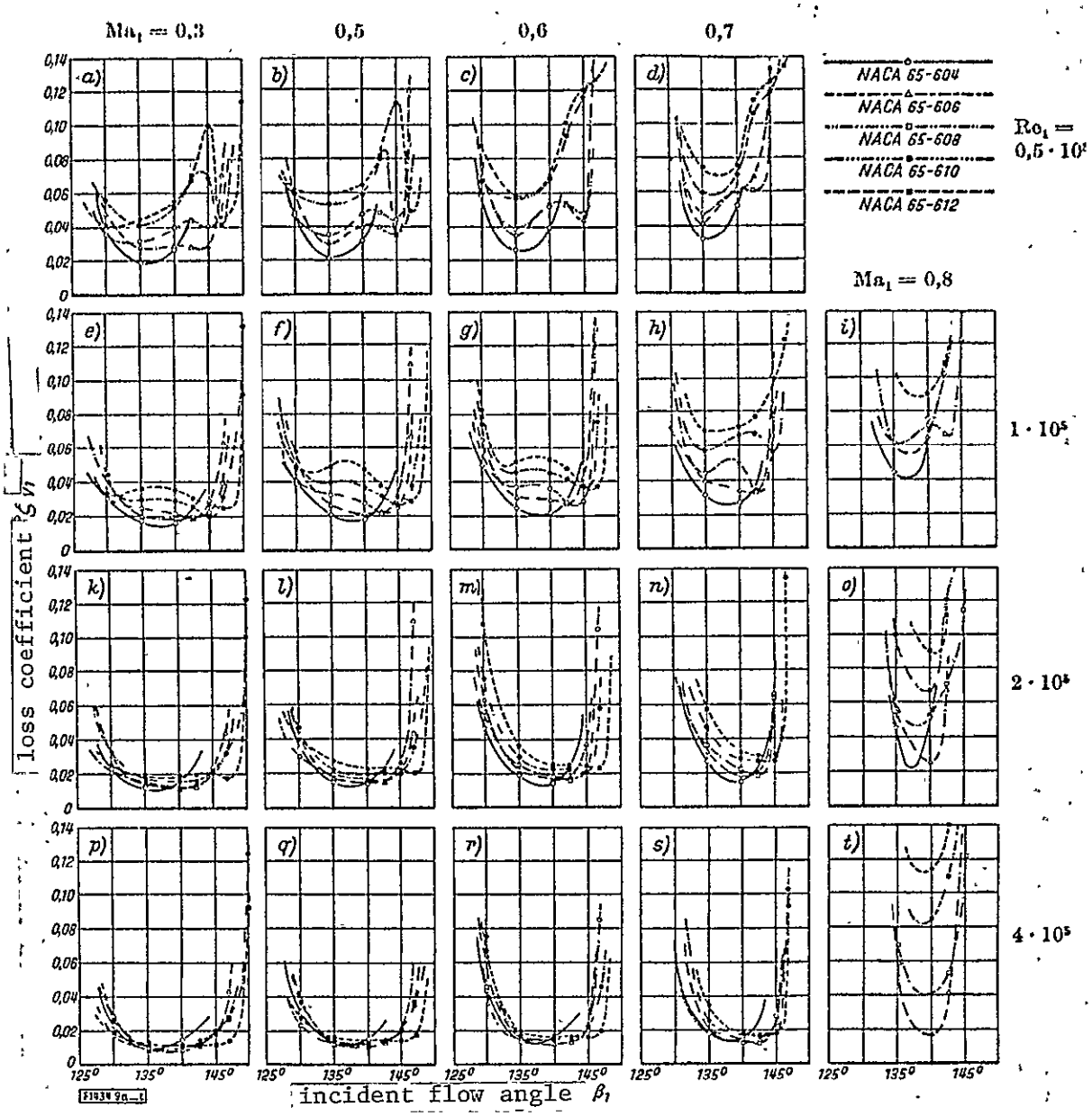

Figure 9a - 9t: Influence of profile thickness on cascade polars for various values of the incident Reynolds number Re_i and the incident Mach number Ma_i.

Division ratio and blade angle as in Figures 8a - 8e; a) to d) - polars for $Re_i = 0.5 \times 10^5$ for $Ma_i = 0.30$, 0.50, 0.60, or 0.70; e) to i) - polars for $Re_i = 1 \times 10^4$ at $Ma_i = 0.30$, 0.50, 0.60, 0.70, or 0.80; k) to o) - polars for $Re_i = 2 \times 10^4$ for Ma_i, like in e) to i); p) to t), polars for $Re_i = 4 \times 10^5$ for Ma_i as in e) to i).

At even greater incident flow angles, the losses increase again because of the beginning trailing edge separation.

By reducing the Reynolds number to $Re_1 = 2 \times 10^5$ the transition point of the separated laminar boundary layer migrates downstream, whereas the separation point is independent of the Reynolds number at the same point, as shown in Figure 8. In general the bubbles become larger, so that the influence of profile thickness can develop to a high degree. We will discuss why the loss coefficient changes so much with a profile thickness; for example, $Re_1 = 1 \times 10^5$. If we compare the pressure distributions of the profiles of various thickness for an average incident flow angle, Figure 10a, then one finds a large change in the pressure distribution and therefore in the boundary layer flow, both on the suction side and the pressure side. The size of the bubble increases with increasing profile thickness. The separation point migrates upstream, whereas the reattachment point changes hardly at all. In addition to this purely geometric change in the bubble, the loss is determined essentially by the pressure increase in the reattachment point region, which increases greatly with increasing profile thickness. The consequences of an increased pressure increase are thicker boundary layers and therefore higher losses. At large incident flow angles, /20 the processes onthe blade suction side primarily determine the behavior of the cascade shown in Figure 10b. The incident flow angle in this example also lies in a range in which thin profiles have especially high losses due to the excessive cascade angle of attack (see Figure 9e) for $Re_1 = 1 \times 10^5$, $Ma_1 = 0.30$ at $\beta_1 = 147°$. The pressure distributions in Figure 10b can be used to derive the following boundary layer behavior. The pressure variation on the profile underside remains almost independent of profile thickness. The boundary layer is laminar. On the other hand, on the suction side, there is a small separation bubble in the case of the thickest profile ($d/l = 0.12$). The laminar incident boundary layer keeps the loss small. The next thinner profile ($d/l = 0.10$) has a completely turbulent boundary layer, which is associated with higher losses. The even greater loss coefficient for $d/l = 0.08$ is based on the beginning turbulent trailing edge separation.

The Reynolds number $Re_1 = 0.5 \times 10^5$ is so small that there is no longer a bubble in the region of the central polar, because the transition occurs too far downstream. This completely laminar boundary layer separation is intensified with increasing cascade angle of attack, and

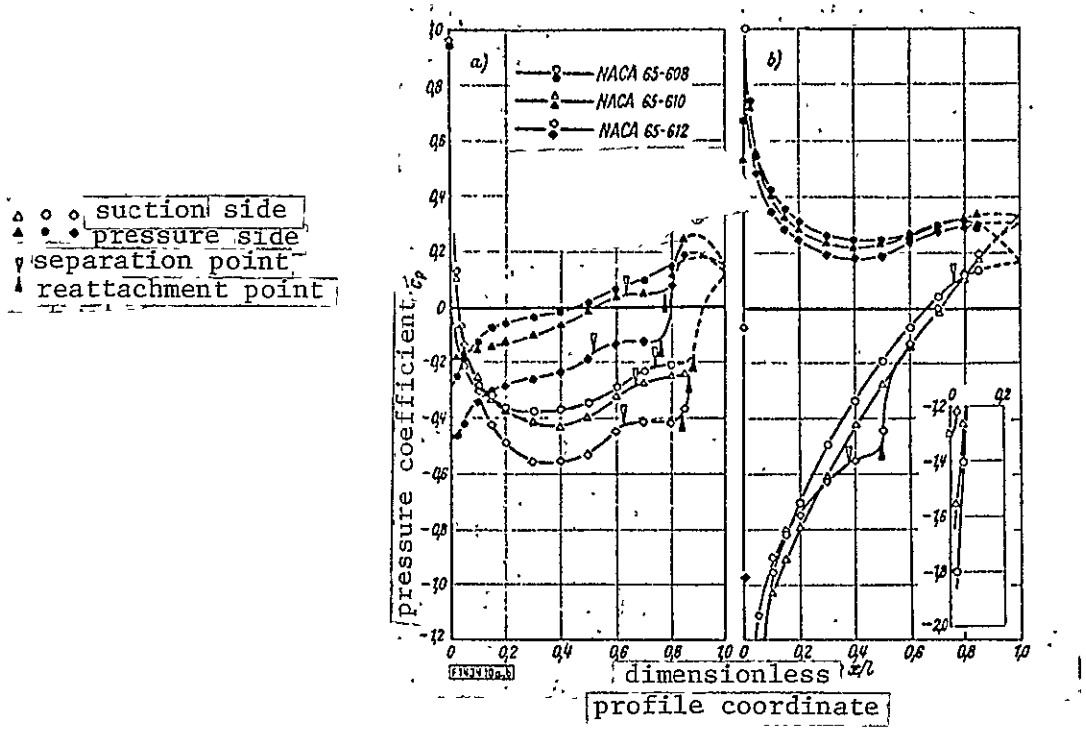

Figure 10a - 10b: Influence of profile thickness on the pressure distribution around the profile characterized by the pressure coefficient c_p according to Eq. (9).

Division ratio t/l, blade angle $\beta_s = 130°$, incident flow Reynolds number $Re_i = 1 \times 10^4$, incident Mach number $Ma_i = 0.30$. a) pressure distribution for average blade load, incident flow angle $\beta_1 = 135°$, b) pressure distribution for large blade load ($\beta_1 = 147°$).

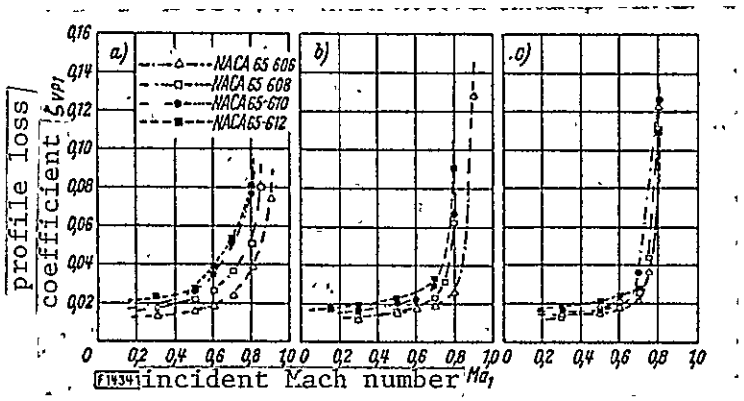

Figure 11a - 11c: Dependence of thickness influence on the profile loss coefficient ζ_{VP1} on the division ratio t/l.

Blade angle $\beta_s = 130°$, incident flow angle $\beta_1 = 140°$, division ratio $Re_i = 2 \times 10^5$; a) to e) - results for t/l = 0.75, 1 and 1.25.

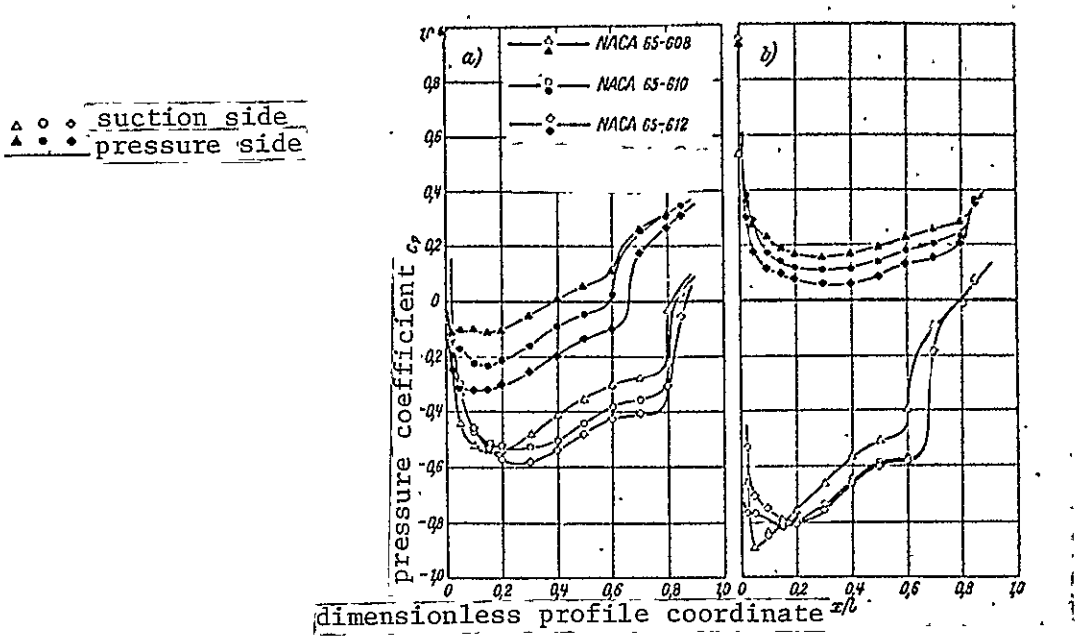

Figures 12a - 12b: Change of the Pressure distribution around the profile, with thickness at various division ratios t/l, characterized by the pressure coefficient c_p, given by Eq. (9). Blade angle β_s = 130°, incident flow angle β_1 = 140°, incident Reynolds number Re_i = 2 x 10^5, incident Mach number, Ma_i = 0.60; a) - b) - for t/l = 0.75 and 1.25.

results in very high losses. The transition-enhancing effect of /21
the suction peaks only becomes effective at relatively high incident flow angles, compared with Re_1 = 1 x 10^5, and this results in a sudden and sometimes substantial decrease in the loss coefficient. If the incident flow angle is increased further, the loss is increased because of the turbulent trailing edge separation.

The previously-described processes only depend on Mach number to the extent that with increasing Ma_1 the separation point migrates upstream, so that the loss coefficients in general increase. After the critical Mach numbers are exceeded, the boundary layers are disturbed by the compression shocks, which leads to very high losses. The critical Mach number depends on the incident flow angle. Because the polars are reached more easily in the vicinity of the profile nose than in the central part, because of the large suction peaks, the polars become narrower.

Finally, let us discuss the influence of the profile thickness

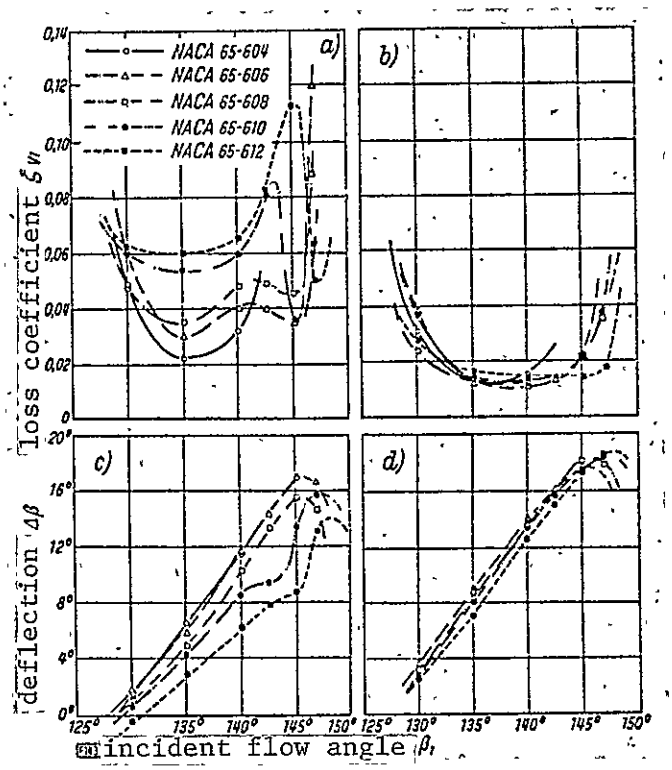

Figures 13a - 13d: Comparison of the Influence of profile thickness on the loss coefficient ζ_{V1} and the deflection $\Delta\beta$ Blade angle $\beta_s = 130°$, division ratio t/l = 1, incident Mach number $Ma_1 = 0.50$; a) and b) - loss coefficient for incident Reynolds numbers, $Re_1 = 0.5 \times 10^4$, or 4×10^5; c) and d) - deflection at $Re_1 = 0.5 \times 10^5$ or 4×10^5.

when there is a changing division. It is appropriate to use equation (8), the profile loss coefficient ζ_{VP1} which does not depend on the division ratio t/l.

As t/l increases, the polar of a blade cascade becomes narrower in general [9]. This is a consequence of a reduced guidance of the flow in the cascade. Considering our investigation, one can raise /22 the question whether for average incident flow angles (in the range of incident flow without shocks), the change in the division has an effect. As long as there are no or very small separation bubbles at sufficiently high Reynolds numbers, the influence of the profile thickness for the most part will remain independent of the division ratio. It is only at smaller Reynolds numbers that the influence becomes substantially greater with decreasing division, as the plot of ζ_{VP1} versus Ma_1 shows, where profile thickness is a parameter, for

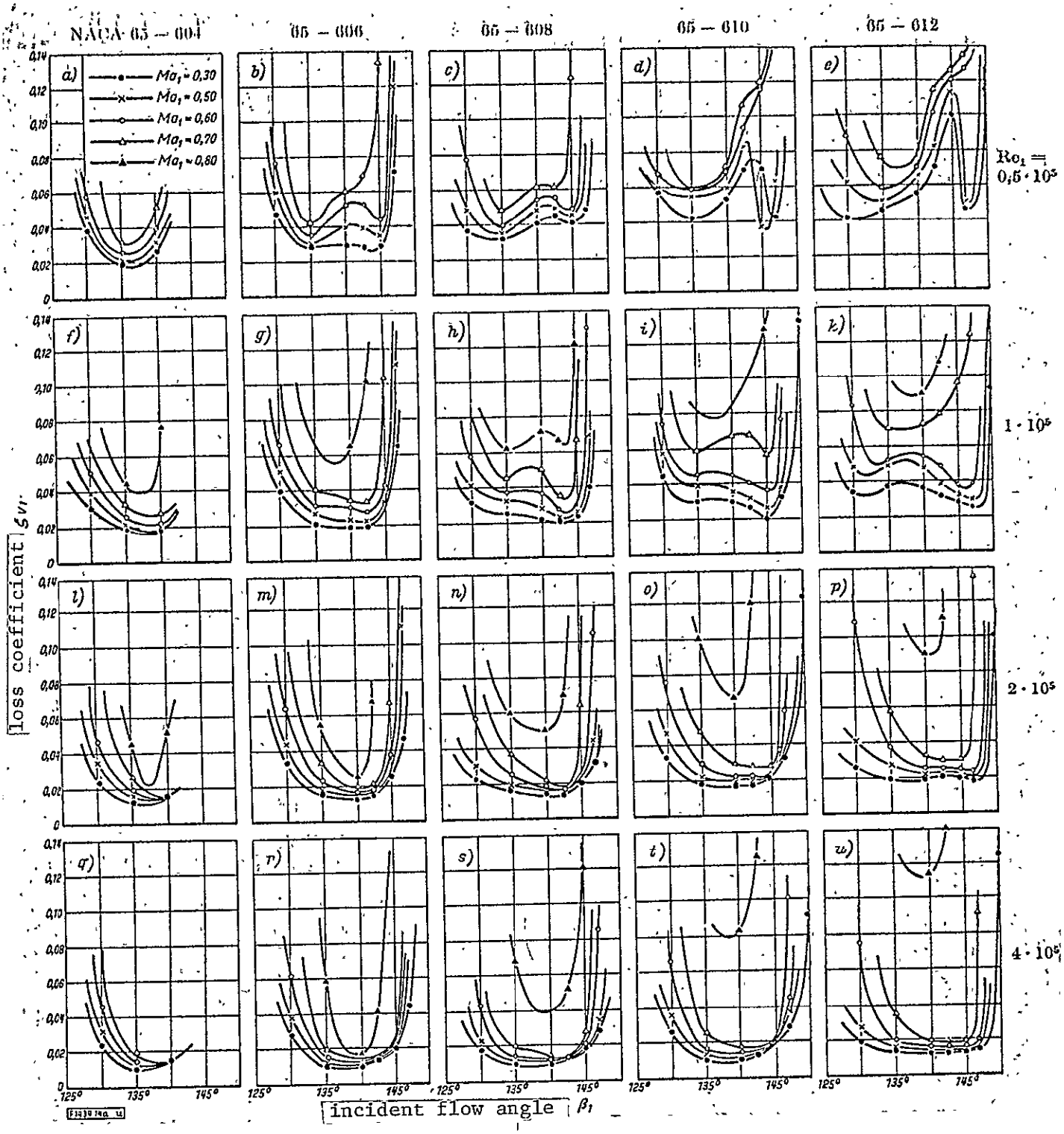

Figure 14a - 14u: Cascade polars of the investigated profiles in a plane compressor cascade with the incident Mach number Ma_1 as a parameter for various incident Reynolds numbers Re_1.

Division ratio t/l = 1, blade angle β_s = 130°; a) to e), at Re_1 = 0.5×10^4 for Profiles NACA 65-604, 65-606, 65-608, 65-610, and 65-612; f) to k) - at $Re_1 \times 1 \times 10^5$ for profiles as in a) to e); l) to p) at $Re_1 = 2 \times 10^5$ for profiles as in a) to e); q) to u)- at $Re_1 = 4 \times 10^5$ for the profiles as in a) to e).

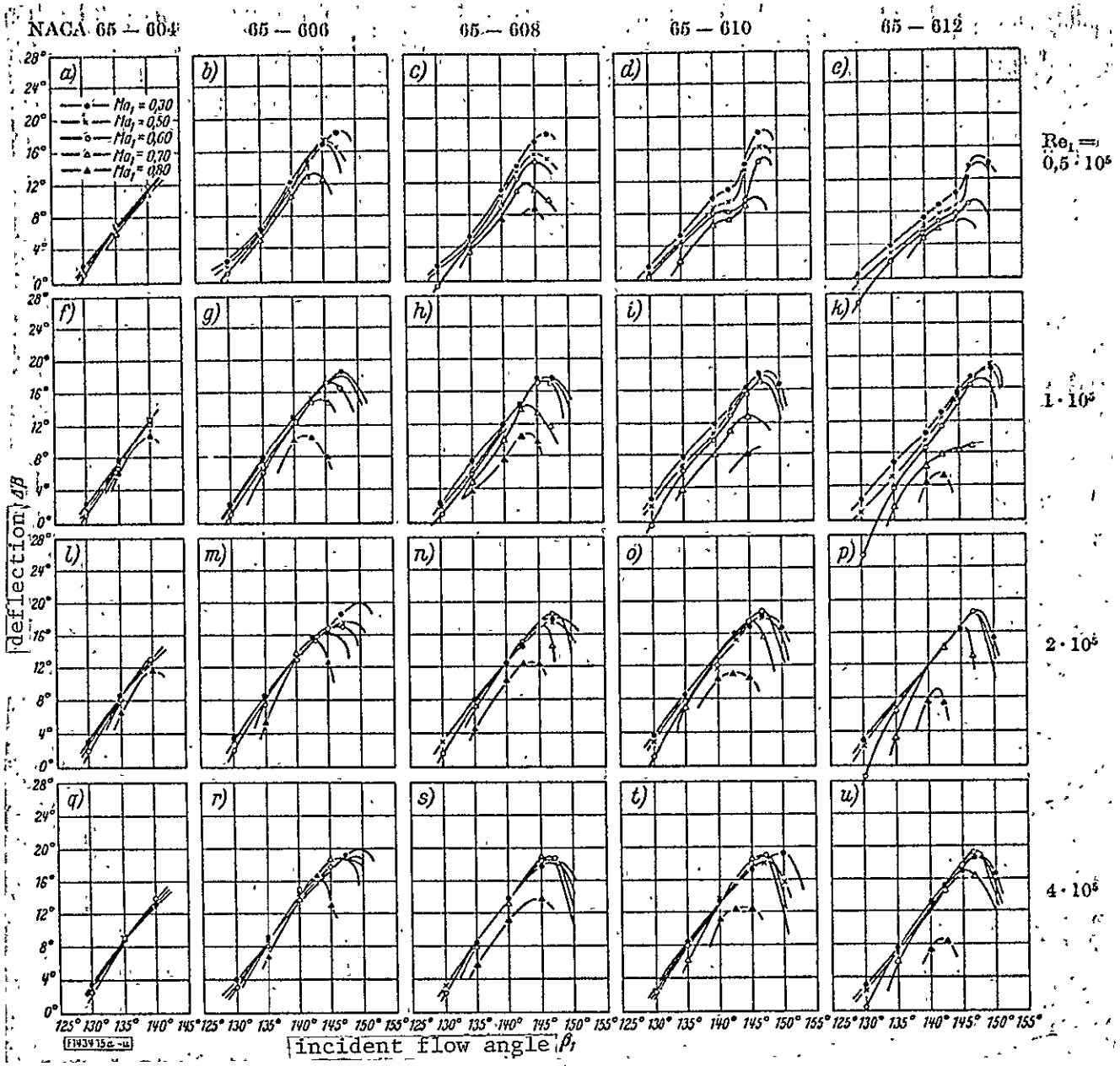

Figure 15a - 15u: Deflection $\Delta\beta$ of the investigated profiles in a plane compressor cascade with the incident Mach number Ma_1 as a parameter for different incident Reynolds number Re_1.

Caption same as in Figures 14a - 14u.

different division ratios (Figure 11a - 11c). In the flow channels which are narrow for small division values, a change in the profile thickness brings about a greater change in the velocity distribution or pressure distribution than for a large blade separation (Figures 12a - 12b). This has a special effect on the pressure jump in the region of the reattachment point of the separated boundary layer, which

itself has a great influence on the thickness of the reattached boundary layer, and on the losses.

2.23 Influence of Profile Thickness on the Deflection: One can establish a direct relationship between the loss coefficient and the departing flow angle, that is, the deflection, by consideration of the processes in the boundary layers. Figures 13a - 13d give an example of the loss coefficient ζ_{v1} and the deflection $\Delta\beta = \beta_1 - \beta_2$ for one Mach number and two Reynolds numbers. It follows from this that there is a large influence of the profile thickness on the losses, and for the deflection as well ($Re_1 = -.5 \times 10^5$). It is found that large losses are connected with small deflections, and vice-versa. If the loss coefficient depends slightly on the profile thickness, the changes in the deflection also remain small ($Re_1 = 0[.4] \times 10^5$).

2.24 Influence of Mach Number and Reynolds Number on aerodynamic coefficients: Figures 14a to 14u and 15a to 15u show the cascade polars and the deflections of the five investigated profiles with Mach number as a parameter of the different Reynolds numbers. The influence of Ma_1 and Re_1 was already discussed in journal terms, in section 2.21, so that we do not have to give a detailed discussion of Figures 14a to 14u and 15a to 15u.

2.25 Influence of Profile Thickness on Critical Mach number. By critical Mach number Ma_{1kr}, we understand the value of Ma_1, for which the speed of sound is reached locally over the profile. Above the critical Mach number, there are supersonic fields with compression shocks, which have a great influence on the boundary layers and lead to increased losses.

In order to determine Ma_{1kr}, the smallest pressure $p_{min}(x)$ over the profile must be known. It can be found from the pressure distribution (Figures 16a and b). If one plots the values for the smallest pressure coefficient $c_{pmin} = [p_{min}(x) - p_1]/q_1$ according to Figure 17 as a function of Mach number, then the critical Mach number is found as the intersection point with the curve $c_{pkr} = f(Ma_1)$ according to equation (10).

Figures 18a to 18c show Ma_{1kr} for three profiles as a function of incident flow angle for different Reynolds numbers. In the range of incident flow without shocks, ($\beta_1 \approx 140°$), the curves have a maximum because here the pressure distributions havethe smallest suction peaks.

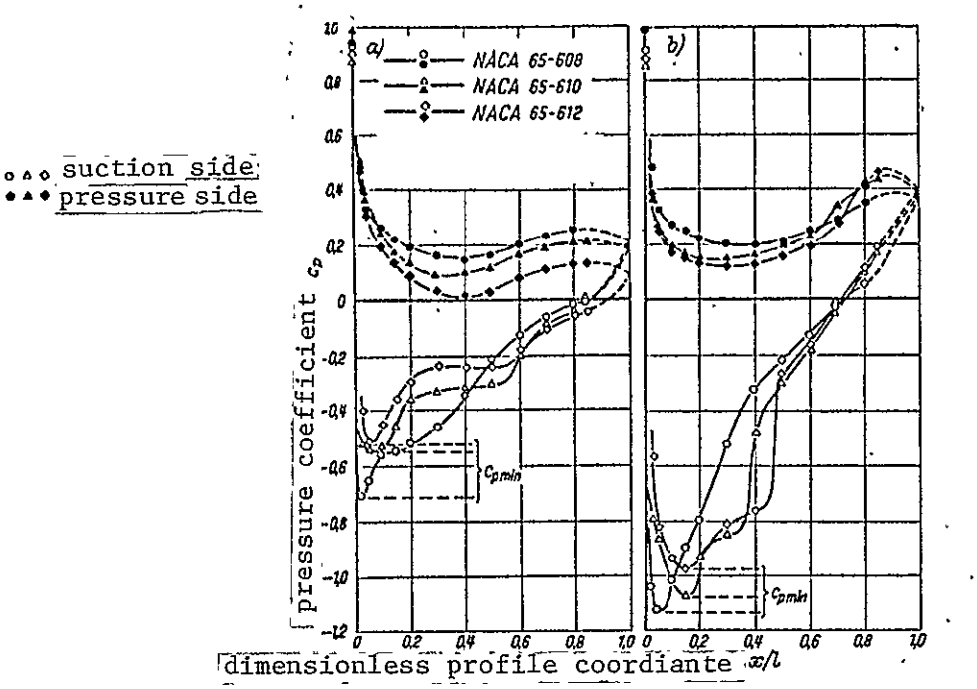

Figure 16a - 16b: Determination of the smallest pressure coefficient c_{pmin} from the dimensionless pressure distribution around the profile. Division ratio t/l = 1, blade angle β_s = 130°, incident flow angle β_1 = 140°, incident Mach number Ma_1 = 0.50; a) and b) = for the incident Reynolds numbers Re_1 = 1 x 10^5 and 4 x 10^5.

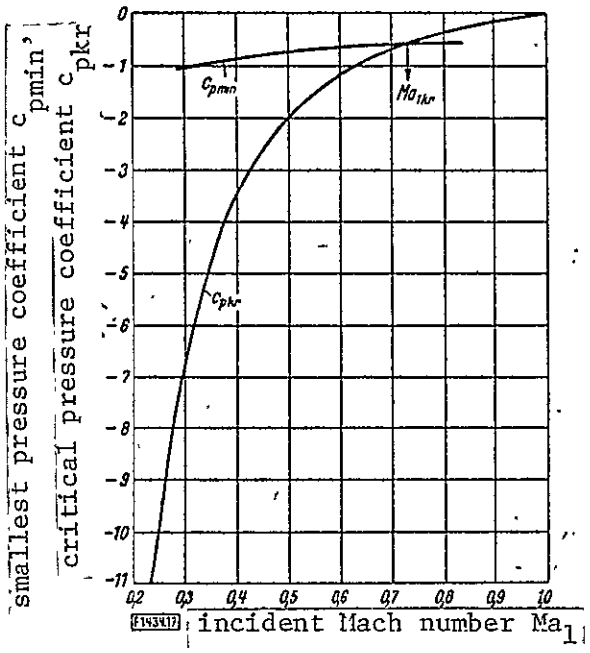

Figure 17: Example for determining the critical incident flow Mach number Ma_{1kr} from the dimensionless pressure coefficient around the profile.

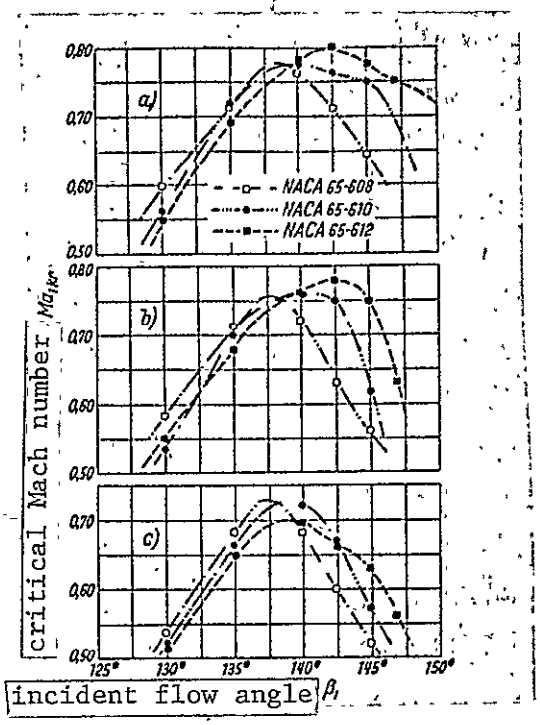

Figures 18a - 18c: Influence of profile thickness on the critical Mach number Ma_{1kr} as a function of the incident flow angle β_1 for different Reynolds numbers Re_1.
Division ratio t/l = 1, blade angle β_s = 130°,
a) to c) - for Re_1 = 0.5 x 10^5, 1x10^5 or 4 x 10^5.

There is only a large influence of the profile thickness for large incident flow angles, compared with the angle for incident flow without shocks. The critical Mach number, therefore, decreases with decreasing profile thickness. This is because the smaller nose radii of the thin profiles produce higher suction peaks in the flow around the blade leading edge.

As the Reynolds number decreases, Ma_{1kr} increases. This is due to the effect of boundary layer separation, which influences the flow upstream in such a manner that the suction peaks are reduced (Figure 16a and 16b). The more extensive the separations, the greater will be their influence.

3. THEORETICAL ANALYSIS

3.1 Computer Program

The theoretical analysis of the laminar separation bubbles, which have a substantial influence on the flow through a blade cascade for

Table 2: Computer Program.

Investigated Quantity	Profile NACA 65-604, NACA 65-608, NACA 65-612
Blade angle β_s	130°
Division ratio t/l	1
Incident Flow Angle β_1	135°, 140°, 145°, 150°
Mach number Ma_1	0, 0.4, 0.8

small Reynolds numbers cannot yet be performed. In the following, we will only show that based on potential theory pressure distributions, in conjunction with experimental results, one can derive information about the occurrence of separation bubbles and predict the behavior of blade cascades when individual cascade profile parameters are changed. Using the methods of H. Schlichting [30], as well as H. Schlichting /24 and E. G. Feindt [13], we calculated pressure distributions. In the first case, this is a singularity method for incompressible flow. The second method is based on the use of the Prandtl-Glauert rule, for the cascade, and considers the influence of compressibility at high subsonic velocities.

3.2 Results

Figures 19a to 19m show the calculated dimensionless pressure distributions where profile thickness is the parameter for different values of β_1 and Ma_1. The substantial influence of profile thickness at small incident flow angles decreases with increasing incident flow angles.

The behaviors of the suction peaks and the pressure gradient are the most important factors for boundary layer separation. The incident flow angle also plays a role here. At a moderate incident flow angle (β_1 = 135° and 140°), the smallest pressures prevail in the center of the blade for the thick profiles. Since the pressure gradients in this case remained relatively small, one would only expect a noticeable influence of profile thickness when laminar boundary layers occur over the blades at Reynolds numbers (see Figures 9a to 9t for $Re_1 < 2 \times 10^5$). Laminar boundary layers are very sensitive to increasing pressure. They

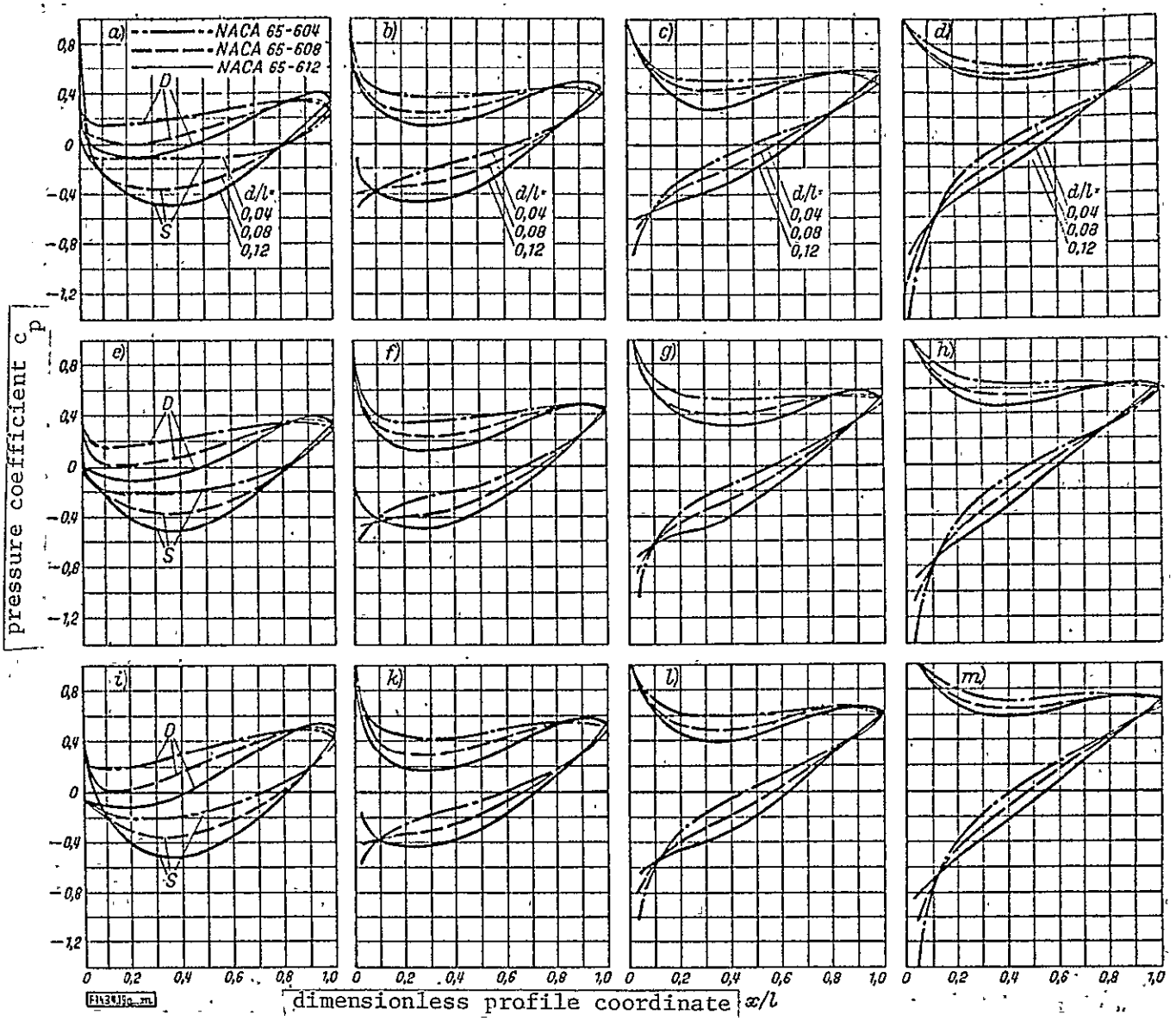

Figures 19a - 19m: Calculated dimensionless pressure distributions around the profile for pure potential flow for different profile thicknesses, different incident flow angles β_1 and different incident Mach numbers Ma_1.

Division ratio t/l = 1, blade angle β_s = 130°, d- maximal profile thickness; l- blade chord, D and S- variation on the pressure and suction side; a) - d) - for Ma_1 = 0 at β_1 = 135, 140°, 145° and 150°, e) - h), for Ma_1 = 0.4 at β_1 according to a) and d); i) - m) - for Ma_1 = 0.8, for β_1 according to a) and d).

have a greater tendency to separate from thick profiles than from thin profiles. In addition, the wake becomes wider because of the greater pressure increase and produces higher losses. At high Reynolds numbers, Figure 9a to 9t for $Re_1 = 4 \times 10^5$, where the boundary layers are turbulent

at least downstream from the suction peak, and therefore produce substantially greater pressure increases, there is hardly any influence of a change in profile thickness.

If one increases the incident flow angle, then the suction peaks will appear in the leading edge area because of the sharp flow around the profile nose. Now, one finds that the thinner profiles produce the greater suction peaks because of their pointed noses. Related to this are the very great pressure increases, which make laminar boundary layers undergo transition and which make turbulent boundary layers separate. For large cascade angles of attack, this means that thin /25
profiles are in much greater danger of separation. The Reynolds number plays no role here because the extremely sharp suction peaks result in turbulent boundary layers even for low Reynolds numbers.

4. REFERENCES

1. Riegels, F. W.: Aerodynamische Profile (Aerodynamic Profiles). Munchen;, R. Oldenbourg 1958.

2. Abbott, I. H., and Von Doenhoff, A. E.: Theory of wing sections. New York: McGraw Hill Book Company, Inc., 1949.

3. Herrig, L. J., Emery, J. C., and Erwin, J. R.: Effect of section Thickness and trailing-edge radius on the performance of NACA 65-series compressor blades in cascade at low speeds. Nat. adv. Comm. Aeron. (NACA), RM Nr. L 51 J 16. Washington, 1951.

4. Held, W.: The design of Delay Cascades of Axial Turbo-machines using simple approximate relationships. Technik 14 (1959), Nr. I S, 3/10.

5. Eckert, B.: Axialkompressoren und Radialkompressoren (Axial compressors and Radial Compressors), Berlin-Goettingen-Heidelberg; Springer-Verlag 1953.

6. Erwin, J. R., Savage, M., and Emery, J. C.: Two-dimensional low speed cascade investigation of NACA compressor blade sections having a systematic variation in meanline loading. Nat. Adv. Comm. Aeron. (NACA), TN Nv. 3817, Washington, 1956.

7. Herrig., L. J., Emery, J. C., and Erwin, J. R.: Systematic two-dimensional cascade tests of NACA 65-series compressor blades at low speeds. Nat. adv. Comm. Aeron. (NACA) TN Nr. 3916. Washington, 1957.

8. Emery, J. C.: Low-Speed cascade investigation of compressor blades

having loaded leading-edges. Nat. adv. Comm. Aeron. (NACA), Tn nr. 4178, Washington, 1958.

9. Schlichting, H.: Application of Boundary Layer Theory to Flow Problems in Turbo-machines. Siemens - Z. 33 (1959), Nr. 7 S 429/38.

10. Grewe, K. H.: Pressure distribution measurements and theoretical comparison calculations for plane blade cascades at high subsonic velocities. Forsch. Ing.-Wes. 25 (1959), Nr. 1, p. 1-16.

11. Hopkes, U.: Influence of Mach number for plane blade cascade flows, wake measurements and comparison calculations at high subsonic velocities. Forsch.-Ing. Wes. 26 (1960), Nr. 5, p. 141-52.

12. Lindner, E., Langer, L. and Bahr, A.: Flow properties of straight blade cascades for compressible flow. Technik 16 (1961), Nr. 6, p. 441-45, Nr. 7, p. 505-509, and Nr. 8, p. 575-578.

13. Schlichting, H., and Feindt, E. G.: Calculation of frictionless flow for a prescribed plane blade cascade at high subsonic velocities. Forsch. Ing.-Wes. 24 (1958), Nr. 1, p. 19-28.

14. Adams, E.: Application of the Karman-Tsien rule to plane compressible cascade flows in the subsonic range. Inst. f. Aerodynamik d. Dtsch. Forschungsanst. fur Luft- u. Raumfahrt Braunschweig, 1956. (Report 56/31)

15. Oswatitsch, K., and Ryhming, J.: The compressibility influence of plane blade cascades with high deflection. Ber. 28 d. Deutschen Versuchsanstalt f. Luftfahrt, Mulheim (Ruhr), 1957.

16. Uchida, S.: Calculation of compressible cascade flow by the method of flux analysis. J. Aeron. Sci. 21 (1954), Nr. 4, p. 237-250.

17. Emery, J. C., and Dunavant, J. C.: Two-dimensional cascade tests of NACA-65-($c_{l_0}A_{l_0}$) 10 blade sections of typical compressor hub conditions for speeds up to choking. Nat. Adv. Comm. Aeron. (NACA) RM Nr. L 57 H 05, Washington, 1957.

18. Aircraft Propulsion Data Book. Aircraft Gas Turbines Division General Electric. Cincinnati, Ohio, 1956.

19. Schmitz, F. W.: Aerodynamik des Flugmodells. Duisburg, C. Lange 1960.

20. Abbott, I. H., Von Doenhoff, A. E., and Stivers, L. S., Summary of airfoil data. Nat. Adv. Comm. Aeron. (NACA), TR Nr. 824. Washington, 1954.

21. Schlichting, H.: The variable density high speed cascade wind tunnel of the Deutsche Forschungsanstalt fur Luftfahrt Braunschweig. AGARD-Report Nr. 91 der Advisory Group for Aeron. Res. and Development. Paris, 1956.

22. Scholz, N., and Hopkes, U.: High velocity cascade wind tunnel of the German Research Facility for Aviation, Braunschweig. Forsch. Ing.-Wes. 25 (1959), Nr. 5, p. 133-147.

23. Scholz, N.: Systematic Measurement for plane blade cascades. Z. Flugwiss, 4 (1956), Nr. 10, p. 313-333.

24. Parr, O.: Measurement of the degree of turbulence in the wind tunnels of the Institute for Fluid Mechanics of the Technical University, Braunschweig, and the Institute for Aerodynamics of the DFL. Report 60/14 of the Inst. f. Stromungsmechanik der Techn. Hochschule Braunschweig, 1960. See also Hebbel, H. H.: Influence of Mach number and Reynolds number on the degree of turbulence of the high velocity cascade wind tunnel. Report 62/22 of the Inst. f. Aerodyanmik der Deutschen Forschungsanstalt fur Luft- and Raumfahrt Braunschweig, 1962.

25. Hebbel, H. H. Influence of Mach number and Reynolds number on Aerodynamic Parmaters of turbine blade cascades for different degrees of turbulence in the flow. Diss. Techn. Hochschule Braunschweig, 1962. Will appear soon in this journal.

26. Kynast, G.: Evaluation of wake measurements over blade cascades for compressible flow. To appear soon in this journal.

27. Schlichting, H.: Grenzschicht-Theorie. (Boundary Layer Theory), 3rd Edition, Karlsruhe, G. Braun. 1958.

28. Bursnall, W. J., and Loftin, L. K.: Experimental Investigation of localized regions of laminar boundary-layer separation. Nat. Adv. Comm. Aeron., (NACA), TN Nr. 2338, Washington, 1951.

29. Gruschwitz, E.: Approximate calculation of the laminar boundary layer in compressible flow over a non-heat conducting wall. Report No. 47 of the Office National d'Etudes et de Recherches Aeronautique (ONERA), Paris, 1950).

30. Schlichting, H.: Calculation of frictionless incompressible flow for a prescribed plane blade cascade. VDE-Research Report 447, Dusseldorf, VDI-Verlag, 1955.